IEEE Access
Multidisciplinary ⋮ Rapid Review ⋮ Open Access Journal

Received 28 January 2023, accepted 21 February 2023, date of publication 2 March 2023, date of current version 29 March 2023.

Digital Object Identifier 10.1109/ACCESS.2023.3251726

RESEARCH ARTICLE

Limited Feedback Design Based on Kronecker Product Codebook for Massive MIMO Systems

KYUNGSIK MIN[1] AND TAEHYOUNG KIM[2], (Member, IEEE)
[1]Department of Information and Telecommunications Engineering, The University of Suwon, Hwaseong 18323, South Korea
[2]Department of Information and Communication Engineering, Soonchunhyang University, Asan 31538, South Korea

Corresponding author: Taehyoung Kim (th.kim@sch.ac.kr)

This work was supported in part by the Soonchunhyang University Research Fund, and in part by the National Research Foundation of Korea (NRF) Grant through the Korea Government [Ministry of Science and Information and Communication Technology (MSIT)] under Grant NRF-2022R1F1A1064106.

ABSTRACT To realize massive multiple-input multiple-output (MIMO) systems, the uniform planar array (UPA) structure has been adopted to deploy a large number of antennas in a limited area of a radio unit at a base station. Subsequently, the Kronecker product (KP) codebook, consisting of horizontal and vertical-domain codebooks, was introduced to enable efficient quantization and feedback for the channel state information (CSI) under the UPA structure. In this paper, we propose advanced limited feedback schemes based on the KP codebook for massive MIMO systems. First, we propose one feedback bit allocation scheme to maximize the beamforming gain. Eigenvalues of spatial correlation channels are used to determine the numbers of feedback bits for horizontal and vertical-domain CSI, and the numbers of feedback bits to maximize the beamforming gain are derived as a closed-form expression. Moreover, we propose a novel feedback and pilot transmission scheme to reduce both the feedback and pilot overhead. The proposed feedback and pilot transmission scheme utilizes the property that the small-scale fading information can be compressed only to the horizontal-domain CSI when the spatial correlation of the vertical-domain channel is high. Simulation results show that, with the use of the proposed feedback bit allocation, the beamforming gain increases by up to 65% compared with the fixed feedback bit allocation when the horizontal and vertical-domain spatial correlation coefficients are equal to 0.57, and the numbers of horizontal and vertical-domain antennas are 8 and 12, respectively. In addition, it is also shown that the proposed feedback and pilot transmission scheme improves the ergodic rate by up to 48% compared with conventional feedback schemes.

INDEX TERMS KP codebook, limited feedback, massive MIMO, UPA.

I. INTRODUCTION

Multiple-input multiple-output (MIMO) is a key technology to accommodate the explosive growth of mobile data traffic by improving the capacity of wireless communication systems. In particular, in the fifth-generation (5G) mobile communications, massive MIMO systems have been commercialized globally at a rapid speed [1]. A large number of antennas in massive MIMO systems enables simultaneous support of multiple users in the same time-frequency resource by spatial-domain multiplexing, which results in achieving high spectral efficiency [2]. The capability to provide services to multiple users makes massive MIMO systems attractive to both academia and industry.

The performance of massive MIMO systems depends heavily on the accuracy of the channel state information (CSI) [3]. In this regard, the time division duplex (TDD) mode is preferred for its merit of acquiring CSI accurately thanks to channel reciprocity. With channel reciprocity, the downlink CSI can be obtained with simple conjugate and transpose operations of the uplink channel estimate. However, the TDD mode is only allowed to operate in the specific frequency bands that are agreed upon by an international standard group, such as the international telecommunication

The associate editor coordinating the review of this manuscript and approving it for publication was Wei Feng.

This work is licensed under a Creative Commons Attribution-NonCommercial-NoDerivatives 4.0 License.
For more information, see https://creativecommons.org/licenses/by-nc-nd/4.0/

union or the 3rd generation partnership project (3GPP) [4]. Therefore, massive MIMO systems can operate in the frequency division duplex (FDD) mode in some frequency bands, where the accurate CSI is difficult to be obtained compared with the TDD mode. To improve the accuracy of CSI in the FDD mode, a downlink training method was proposed in [5] where long-term channel statistics and previously received training signals from users are utilized. In [6], Bayesian learning-based channel estimation that enables the estimation of the downlink channel at the base station (BS) was proposed for the FDD multiuser MIMO system. In addition, partial reciprocity-based CSI acquisition was recently studied [7], [8]. The authors of [7] concluded that the downlink channel can be reconstructed accurately with the aid of an uplink pilot. Furthermore, the authors of [8] proposed a channel prediction framework by tracking time-varying partial CSI, such as angle, delay, and Doppler information.

Meanwhile, to obtain the downlink CSI at the BS, closed-loop feedback can be utilized, where the downlink CSI is measured and sent by the user. To report the downlink CSI from the user to the BS, a codebook, which is the set of codewords predefined between the BS and user, is typically utilized [9]. A well-designed codebook can improve the performance of FDD massive MIMO systems [10], [11], [12], [13]. A weighted codebook with a spatial correlation matrix improves the performance by biasing the direction of codewords towards the direction that considers the spatial correlation [10]. Furthermore, codebook designs that are tailored for multiuser MIMO can achieve performance gain by considering multiuser interference mitigation in designing codebook [11]. Recently, machine learning and reinforcement learning-aided CSI quantization have been widely investigated owing to their high quantization performance and robustness to channel variations [12], [13].

To realize a commercial product for massive MIMO systems, a uniform planar array (UPA) structure was proposed to deploy a large number of antennas in a limited area [14]. In the UPA structure, the spatial correlation matrix can be decomposed into horizontal and vertical-domain spatial matrices [15]. The decomposable spatial correlation matrix allows the Kronecker product (KP) codebook, which consists of two separate codebooks for horizontal and vertical-domain spatial correlation matrices [16], [17]. Many prior works have studied KP codebook design and proposed feedback algorithms based on the KP codebook [16], [17], [18], [19], [20], [21], [22], [23], [24], [25]. The authors of [16] proposed dividing the feedback of the precoder into horizontal and vertical-domain precoders based on the discrete Fourier transform (DFT) codebook. The authors of [17] showed that the spatial correlation matrix with the UPA structure at the BS can be decomposed into horizontal and vertical-domain spatial correlation matrices. The low feedback overhead for the KP codebook was addressed by [18] and [19]. In [18], the authors proposed a dynamic adaptation of CSI periodicity considering a slow-varying elevation channel. In [19], a feedback scheme was proposed to reduce codebook resolution for slow-varying horizontal channels. The authors of [20] proposed the selection of multiple DFT codewords for each vertical and horizontal channel. Furthermore, advanced quantization methods were proposed for the KP codebook in [21] and [22]. The authors of [21] proposed a CSI quantization method by quantizing and combining dominant beams for narrowband and wideband. The authors of [22] proposed a codebook design with model-free data-driven approach. In addition, the KP codebook designs compliant to 3GPP standard were investigated in [23], [24], and [25]. In [23], the authors proposed a codebook design based on the linear combination (LC) and the feedback scheme for the LC-based KP codebook. In [24], precoder search algorithms were proposed for Type-I and Type-II codebooks which were defined in 3GPP new radio specification. Further, low-complexity precoder search scheme for Type-II codebook was proposed in [25].

Although prior works in [16], [17], [18], [19], [20], [21], [22], [23], [24], and [25] addressed the KP codebook-based feedback scheme, the quantitative analysis and optimization on the amount of feedback bits have not been studied. Moreover, to the best of our knowledge, a scheme that jointly considers feedback bits and pilot transmission has not been developed.

In this study, we propose a limited feedback design for FDD massive MIMO systems using the UPA structure. The contributions of this study are as follows:

- First, we propose one feedback bit allocation scheme to maximize the average beamforming gain. We analyze the average beamforming gain in terms of the number of feedback bits and eigenvalues of the horizontal and vertical-domain spatial correlation matrices. Based on the analyzed average beamforming gain, we show that the number of feedback bits for the horizontal and vertical-domain precoders are decided based on the relationship between the number of dominant eigenvalues of the horizontal and vertical-domain spatial correlation matrices.
- Next, we propose a feedback and pilot transmission scheme. The proposed feedback scheme can compress the small-scale fading channel information to the horizontal-domain codeword when the spatial correlation of the vertical-domain channel is high. Consequently, the vertical-domain codeword only includes a vertical-domain spatial correlation channel, which does not vary rapidly compared with the small-scale fading channel. Therefore, only the horizontal-domain codeword needs to be reported frequently compared with the vertical-domain CSI. This contributes to reducing both the number of feedback bits and pilot overhead.

The remainder of this paper is organized as follows. In Section II, we describe the system model using KP codebook. In Section III, the feedback bit allocation scheme is proposed. In Section IV, the feedback and pilot transmission schemes for highly correlated vertical-domain channels are

proposed. In Section V, the simulation results of the proposed schemes are presented. Finally, Section VI concludes the paper.

Notation: We use boldface uppercase and lowercase letters for the matrices and vectors, respectively. Operators $(\cdot)^*$, $(\cdot)^T$, and $(\cdot)^H$ denote the conjugate, transpose, and conjugate transpose, respectively. Operators $\|\cdot\|$, $|\cdot|$, and $\otimes$ denote the Euclidean norm, absolute value, and KP, respectively. $\mathbf{I}_K$ denotes a $K \times K$ identity matrix. $\mathbf{0}_{m\times n}$ denotes $m \times n$ matrix with all elements equal to zero. $\mathbf{X}_{[1:n]}$ denotes a matrix that takes the first n column vectors of matrix $\mathbf{X}$. $\mathbb{E}[\cdot]$ denotes the expectation. $\mathcal{CN} \sim (\mu, \sigma^2)$ denotes a complex Gaussian random distribution with mean μ and variance σ^2.

II. SYSTEM MODEL

We consider a downlink system in which the BS and user are equipped with a UPA with $N = N_\mathrm{h} \times N_\mathrm{v}$ antennas and a single antenna, respectively. N_h and N_v are the numbers of antennas in the horizontal and vertical-domains, respectively. Here, data transmission and reception can be modeled as

$$y = \sqrt{p}\mathbf{h}^H\mathbf{f}x + n, \tag{1}$$

where y denotes the received symbol at the user, p denotes the transmission power, $\mathbf{h} \in \mathbb{C}^{N\times 1}$ is the channel vector between the BS and user, $\mathbf{f} \in \mathbb{C}^{N\times 1}$ is the precoding vector, x is the transmitted data symbol with $\mathbb{E}[x^2] = 1$, and n is additive white Gaussian noise with zero mean and variance N_0.

In (1), the channel vector is modeled as $\mathbf{h} = \mathbf{R}^{1/2}\mathbf{g}$, where $\mathbf{R} = \mathbb{E}\left[\mathbf{h}\mathbf{h}^H\right] \in \mathbb{C}^{N\times N}$ denotes a spatial correlation matrix. $\mathbf{g} \in \mathbb{C}^{N\times 1}$ is a vector whose elements are independent and identically distributed Rayleigh fading components with $\mathbb{E}\left[\mathbf{g}\mathbf{g}^H\right] = \mathbf{I}_N$. According to [17], [26], [27], and [28], when the antennas at the BS are placed in a UPA antenna structure, the spatial correlation matrix can be decomposed as follows:

$$\mathbf{R} \approx \mathbf{R}_\mathrm{h} \otimes \mathbf{R}_\mathrm{v}, \tag{2}$$

where $\mathbf{R}_\mathrm{h}$ and $\mathbf{R}_\mathrm{v}$ represent the horizontal and vertical-domain spatial correlation matrices, respectively. We denote the eigen-decompositions of $\mathbf{R}_\mathrm{h}$ and $\mathbf{R}_\mathrm{v}$ by $\mathbf{R}_\mathrm{h} = \mathbf{U}_\mathrm{h}\mathbf{\Lambda}_\mathrm{h}\mathbf{U}_\mathrm{h}^H$ and $\mathbf{R}_\mathrm{v} = \mathbf{U}_\mathrm{v}\mathbf{\Lambda}_\mathrm{v}\mathbf{U}_\mathrm{v}^H$, respectively. Using the Karhunen–Loeve transform [28], [29], $\mathbf{h}$ can be expressed as follows:

$$\mathbf{h} = \left[\left(\mathbf{U}_\mathrm{h}\mathbf{\Lambda}_\mathrm{h}^{1/2}\right) \otimes \left(\mathbf{U}_\mathrm{v}\mathbf{\Lambda}_\mathrm{v}^{1/2}\right)\right]\mathbf{g}. \tag{3}$$

With some manipulation, (3) can be rewritten as the following lemma.

Lemma 1: $\mathbf{h}$ in (3) can be expressed as

$$\mathbf{h} = \sum_{k=1}^{r_\mathrm{v}} \left(\mathbf{h}_{\mathrm{h},k} \otimes \sigma_{\mathrm{v},k}\mathbf{u}_{\mathrm{v},k}\right), \tag{4}$$

where r_v denotes the rank of $\mathbf{R}_\mathrm{v}$, $\sigma_{\mathrm{v},k}$ is the kth dominant singular value of $\mathbf{R}_\mathrm{v}$, $\mathbf{u}_{\mathrm{v},k}$ is the kth column of matrix $\mathbf{U}_\mathrm{v}$, and $\mathbf{h}_{\mathrm{h},k} = \mathbf{U}_\mathrm{h}\mathbf{\Lambda}_\mathrm{h}^{1/2}\mathbf{g}_{\mathrm{h},k}$. In addition,

$$\mathbf{g}_{\mathrm{h},k} = \left[g_k \;\; g_{N_\mathrm{v}+k} \;\; g_{2N_\mathrm{v}+k} \;\; \cdots \;\; g_{(N_\mathrm{h}-1)N_\mathrm{v}+k}\right]^T,$$

where $g_{(i-1)N_\mathrm{v}+k}$ is the ith element of vector $\mathbf{g}_{\mathrm{h},k}$.

Proof: See Appendix A. ∎

In (1), the KP codebook-based precoding was considered [17], [27], [30]. The KP codebook consists of the horizontal codebook $\mathcal{C}_\mathrm{h} = \{\tilde{\mathbf{f}}_\mathrm{h}^1, \tilde{\mathbf{f}}_\mathrm{h}^2, \cdots, \tilde{\mathbf{f}}_\mathrm{h}^{2^{B_\mathrm{h}}}\}$ which represents the horizontal-domain spatial correlation matrix, and the vertical codebook $\mathcal{C}_\mathrm{v} = \{\tilde{\mathbf{f}}_\mathrm{v}^1, \tilde{\mathbf{f}}_\mathrm{v}^2, \cdots, \tilde{\mathbf{f}}_\mathrm{v}^{2^{B_\mathrm{v}}}\}$ which represents the vertical-domain spatial correlation matrix. Here, B_h and B_v are the bit-widths of $\mathcal{C}_\mathrm{h}$ and $\mathcal{C}_\mathrm{v}$, respectively. Subsequently, the precoder $\mathbf{f}$ in (1) is generated by

$$\mathbf{f} = \mathbf{f}_\mathrm{h} \otimes \mathbf{f}_\mathrm{v}, \tag{5}$$

where $\mathbf{f}_\mathrm{h}$ and $\mathbf{f}_\mathrm{v}$ are the horizontal and vertical-domain codewords selected in $\mathcal{C}_\mathrm{h}$ and $\mathcal{C}_\mathrm{v}$, respectively. The horizontal and vertical-domain codewords are selected to maximize the received signal-to-noise ratio (SNR), which can be expressed as in [31] by

$$(\mathbf{f}_\mathrm{h}, \mathbf{f}_\mathrm{v}) = \underset{\tilde{\mathbf{f}}_\mathrm{h}\in\mathcal{C}_\mathrm{h}, \tilde{\mathbf{f}}_\mathrm{v}\in\mathcal{C}_\mathrm{v}}{\arg\max} \left|\mathbf{h}^H\left(\tilde{\mathbf{f}}_\mathrm{h} \otimes \tilde{\mathbf{f}}_\mathrm{v}\right)\right|^2. \tag{6}$$

III. FEEDBACK BIT ALLOCATION FOR KP CODEBOOK

In this section, we propose one feedback bit allocation scheme for the KP codebook to maximize the beamforming gain. In the proposed feedback bit allocation scheme, we adopted the channel-dimension reduction technique in [32] to further reduce the feedback overhead.

A. ANALYSIS OF AVERAGE BEAMFORMING GAIN

The channel dimension can be reduced by considering only the dominant eigenvectors of the spatial correlation matrices [32]. Then, the channel with reduced dimension $\mathbf{h}_L \in \mathbb{C}^{L\times 1}$ can be expressed as

$$\begin{aligned}\mathbf{h}_L &= \left(\mathbf{U}_{\mathrm{h}[1:L_\mathrm{h}]} \otimes \mathbf{U}_{\mathrm{v}[1:L_\mathrm{v}]}\right)\mathbf{h} \\ &= \left[\mathbf{\Lambda}_{\mathrm{h}[1:L_\mathrm{h}]} \otimes \mathbf{\Lambda}_{\mathrm{v}[1:L_\mathrm{v}]}\mathbf{0}_{N\times(N-L_\mathrm{h}L_\mathrm{v})}\right]\mathbf{g},\end{aligned} \tag{7}$$

where $L = L_\mathrm{h} \times L_\mathrm{v}$ denotes the reduced channel dimension. L_h and L_v denote the numbers of ordered eigenvectors of the horizontal and vertical-domain spatial correlation matrices, respectively. Then, the user can determine the horizontal and vertical-domain codewords $\mathbf{f}_{L_\mathrm{h}}$ and $\mathbf{f}_{L_\mathrm{v}}$ that satisfy

$$\left(\mathbf{f}_{L_\mathrm{h}}, \mathbf{f}_{L_\mathrm{v}}\right) = \underset{\tilde{\mathbf{f}}_{L_\mathrm{h}}\in\mathcal{C}_{L_\mathrm{h}}, \tilde{\mathbf{f}}_{L_\mathrm{v}}\in\mathcal{C}_{L_\mathrm{v}}}{\arg\max} \left|\mathbf{h}_L^H\left(\tilde{\mathbf{f}}_{L_\mathrm{h}} \otimes \tilde{\mathbf{f}}_{L_\mathrm{v}}\right)\right|^2, \tag{8}$$

where $\mathcal{C}_{L_\mathrm{h}}$ and $\mathcal{C}_{L_\mathrm{v}}$ are the horizontal and vertical-domain codebooks with L_h and L_v dimensions, respectively. In (8), $\left|\mathbf{h}_L^H\left(\tilde{\mathbf{f}}_\mathrm{h} \otimes \tilde{\mathbf{f}}_\mathrm{v}\right)\right|^2$ can be rewritten as

$$\left|\mathbf{h}_L^H\left(\tilde{\mathbf{f}}_\mathrm{h} \otimes \tilde{\mathbf{f}}_\mathrm{v}\right)\right|^2 = \left|\sum_{k=1}^{L_\mathrm{v}}\left(\mathbf{h}_{L_\mathrm{h},k}^H \otimes \sigma_{\mathrm{v},k}\mathbf{u}_k\right)\left(\tilde{\mathbf{f}}_\mathrm{h} \otimes \tilde{\mathbf{f}}_\mathrm{v}\right)\right|^2$$

$$\overset{(a)}{=}\left|\sum_{k=1}^{L_{\mathrm{v}}}\left(\mathbf{h}_{L_{\mathrm{h}},k}^{H}\tilde{\mathbf{f}}_{\mathrm{h}}\right)\sigma_{\mathrm{v},k}\left(\mathbf{u}_{k}\tilde{\mathbf{f}}_{\mathrm{v}}\right)\right|^{2}$$
$$=\left|\sum_{k=1}^{L_{\mathrm{v}}}\tilde{\mathbf{f}}_{\mathrm{h}}^{T}\mathbf{h}_{L_{\mathrm{h}},k}^{*}\sigma_{\mathrm{v},k}\left(\mathbf{u}_{k}\tilde{\mathbf{f}}_{\mathrm{v}}\right)\right|^{2}$$
$$=\left|\tilde{\mathbf{f}}_{\mathrm{h}}^{T}\left(\sum_{k=1}^{L_{\mathrm{v}}}\sigma_{\mathrm{v},k}\mathbf{h}_{L_{\mathrm{h}},k}^{*}\mathbf{u}_{k}\right)\tilde{\mathbf{f}}_{\mathrm{v}}\right|^{2}, \tag{9}$$

where $(\mathbf{A}\otimes\mathbf{B})(\mathbf{C}\otimes\mathbf{D})=\mathbf{AC}\otimes\mathbf{BD}$ is applied in (a) [33]. In (9), we denote $\tilde{\mathbf{H}}=\sum_{k=1}^{L_{\mathrm{v}}}\sigma_{\mathrm{v},k}\mathbf{h}_{L_{\mathrm{h}},k}^{*}\mathbf{u}_{k}$. Then, (8) can be rewritten as

$$\left(\mathbf{f}_{L_{\mathrm{h}}},\mathbf{f}_{L_{\mathrm{v}}}\right)=\underset{\tilde{\mathbf{f}}_{\mathrm{h}}\in\mathcal{C}_{L_{\mathrm{h}}},\tilde{\mathbf{f}}_{\mathrm{v}}\in\mathcal{C}_{L_{\mathrm{v}}}}{\arg\max}\left|\tilde{\mathbf{f}}_{\mathrm{h}}^{T}\tilde{\mathbf{H}}\tilde{\mathbf{f}}_{\mathrm{v}}\right|^{2}. \tag{10}$$

According to (10), $\mathbf{f}_{L_{\mathrm{h}}}$ and $\mathbf{f}_{L_{\mathrm{v}}}$ can be selected that are the closest to the first left and right singular vectors of $\tilde{\mathbf{H}}$, respectively. Then, denoting the left-dominant singular vector of $\tilde{\mathbf{H}}$ as $\tilde{\mathbf{u}}$ corresponding to the largest singular value and defining α_{h} as the correlation between $\tilde{\mathbf{u}}$ and $\mathbf{f}_{L_{\mathrm{h}}}$ where $0\le\alpha_{\mathrm{h}}\le 1$, $\mathbf{f}_{L_{\mathrm{h}}}$ can be expressed as

$$\mathbf{f}_{L_{\mathrm{h}}}=\alpha_{\mathrm{h}}\tilde{\mathbf{u}}+\sqrt{1-\alpha_{\mathrm{h}}^{2}}\tilde{\mathbf{u}}^{\perp}, \tag{11}$$

where $\tilde{\mathbf{u}}^{\perp}$ denotes a vector orthogonal to $\tilde{\mathbf{u}}$. Similarly, denoting the right-dominant singular vector of $\tilde{\mathbf{H}}$ as $\tilde{\mathbf{v}}$ and defining α_{v} as the correlation between $\tilde{\mathbf{v}}$ and $\mathbf{f}_{L_{\mathrm{v}}}$ where $0\le\alpha_{\mathrm{v}}\le 1$, $\mathbf{f}_{L_{\mathrm{v}}}$ can be expressed as

$$\mathbf{f}_{L_{\mathrm{v}}}=\alpha_{\mathrm{v}}\tilde{\mathbf{v}}+\sqrt{1-\alpha_{\mathrm{v}}^{2}}\tilde{\mathbf{v}}^{\perp}, \tag{12}$$

where $\tilde{\mathbf{v}}^{\perp}$ denotes a vector orthogonal to $\tilde{\mathbf{v}}$. The beamforming gain is defined as

$$\gamma_{L}=\left|\mathbf{h}_{L}^{H}\left(\mathbf{f}_{L_{\mathrm{h}}}\otimes\mathbf{f}_{L_{\mathrm{v}}}\right)\right|^{2}. \tag{13}$$

By substituting (11) and (12) into (13), (13) can be expressed as

$$\gamma_{L}=\left|\tilde{\sigma}_{1}\tilde{\mathbf{u}}^{H}\mathbf{f}_{L_{\mathrm{h}}}\tilde{\mathbf{v}}^{H}\mathbf{f}_{L_{\mathrm{v}}}\right|^{2}$$
$$=\alpha_{\mathrm{h}}^{2}\alpha_{\mathrm{v}}^{2}\tilde{\sigma}_{1}^{2}, \tag{14}$$

where $\tilde{\sigma}_{1}$ denotes the largest singular value of $\tilde{\mathbf{H}}$. Assuming that the horizontal and vertical-domain codebooks are mutually independent and also independent of channel realizations, the average beamforming gain can be expressed as

$$\mathbb{E}\left\{\gamma_{L}\right\}=\mathbb{E}\left\{\alpha_{\mathrm{h}}^{2}\right\}\mathbb{E}\left\{\alpha_{\mathrm{v}}^{2}\right\}\tilde{\sigma}_{1}^{2}. \tag{15}$$

For tractable analysis of the quantization errors, we assume random vector quantization for the horizontal and vertical-domain codebooks [31]. Then, $\mathbb{E}\left\{\alpha_{\mathrm{h}}^{2}\right\}$ and $\mathbb{E}\left\{\alpha_{\mathrm{v}}^{2}\right\}$ can be expressed as

$$\mathbb{E}\left\{\alpha_{\mathrm{h}}^{2}\right\}=1-2^{B_{\mathrm{h}}}\beta\left(2^{B_{\mathrm{h}}},\frac{L_{\mathrm{h}}}{L_{\mathrm{h}}-1}\right) \tag{16}$$

and

$$\mathbb{E}\left\{\alpha_{\mathrm{v}}^{2}\right\}=1-2^{B_{\mathrm{v}}}\beta\left(2^{B_{\mathrm{v}}},\frac{L_{\mathrm{v}}}{L_{\mathrm{v}}-1}\right), \tag{17}$$

respectively. $\beta(a,b)$ represents a beta function with input parameters a and b. Furthermore, to analyze $\tilde{\sigma}_{1}^{2}$, we introduce the following inequality:

$$\left|\mathbf{h}_{L}^{H}\left(\mathbf{f}_{L_{\mathrm{h}}}\otimes\mathbf{f}_{L_{\mathrm{v}}}\right)\right|^{2}<\left\|\mathbf{h}_{L}^{H}\right\|^{2}$$
$$=\left|\sum_{m=1}^{L_{\mathrm{h}}}\sum_{k=1}^{L_{\mathrm{v}}}\sigma_{\mathrm{h},m}\sigma_{\mathrm{v},k}g_{(m-1)N_{\mathrm{v}}+k}\right|^{2}. \tag{18}$$

Based on (18), $\tilde{\sigma}_{1}^{2}$ can be upper bounded such that

$$\tilde{\sigma}_{1}^{2}<\sum_{m=1}^{L_{\mathrm{h}}}\sigma_{\mathrm{h},m}^{2}\sum_{k=1}^{L_{\mathrm{v}}}\sigma_{\mathrm{v},k}^{2}. \tag{19}$$

The equations (15)–(19) show that the average beamforming gain with the KP codebook is upper bounded by the multiplication of correlations for the selected horizontal and vertical-domain codewords and eigenvalues of the horizontal and vertical-domain spatial correlation matrices.

B. PROPOSED FEEDBACK BIT ALLOCATION

Based on (15), we formulate an optimization problem to obtain the numbers of feedback bits maximizing the average beamforming gain given by

$$\underset{L_{\mathrm{h}},L_{\mathrm{v}},B_{\mathrm{h}},B_{\mathrm{v}}}{\text{maximize}}\ \mathbb{E}\left\{\alpha_{\mathrm{h}}^{2}\right\}\mathbb{E}\left\{\alpha_{\mathrm{v}}^{2}\right\}\tilde{\sigma}_{1}^{2} \tag{20a}$$
$$\text{subject to}\quad L_{\mathrm{h}}\in\{1,\cdots,N_{\mathrm{h}}\},L_{\mathrm{v}}\in\{1,\cdots,N_{\mathrm{v}}\}$$
$$B_{\mathrm{h}}\in\{0,\mathbb{Z}\},B_{\mathrm{v}}\in\{0,\mathbb{Z}\},B_{\mathrm{h}}+B_{\mathrm{v}}=B. \tag{20b}$$

The optimal solution of (20a) can be obtained by the exhaustive search method that uses the combinatorial optimization technique [34]. While finding the optimal solution of (20a), the exhaustive search method requires high computational complexity as B, N_{h}, and N_{v} increase. To reduce the complexity, we reformulate the problem in (20a) using the analyzed results. By substituting the upper bound in (19) into (20a), (20a) can be decomposed into

$$\underset{L_{\mathrm{h}},B_{\mathrm{h}}}{\text{maximize}}\ \mathbb{E}\left\{\alpha_{\mathrm{h}}^{2}\right\}\sum_{m=1}^{L_{\mathrm{h}}}\sigma_{\mathrm{h},m}^{2} \tag{21}$$

and

$$\underset{L_{\mathrm{v}},B_{\mathrm{v}}}{\text{maximize}}\ \mathbb{E}\left\{\alpha_{\mathrm{v}}^{2}\right\}\sum_{k=1}^{L_{\mathrm{v}}}\sigma_{\mathrm{v},k}^{2}. \tag{22}$$

The optimal solutions of (21) and (22) can also be obtained by the exhaustive search method. To further reduce the computational complexity, we propose to sequentially find solutions. The proposed method first finds L_{h} and L_{v} followed by B_{h}

and B_{v}. By substituting $B_{\mathrm{h}} = B_{\mathrm{v}} = B/2$ and the approximated results $\mathbb{E}\{\alpha_{\mathrm{h}}\} \approx 1-2^{\frac{-B/2}{L_{\mathrm{h}}-1}}$ and $\mathbb{E}\{\alpha_{\mathrm{v}}\} \approx 1-2^{\frac{-B/2}{L_{\mathrm{v}}-1}}$ [31] into (21) and (22), we obtain

$$\underset{L_{\mathrm{h}}}{\text{maximize}} \left(\sigma_{\mathrm{h},1}^2, \left(1-2^{\frac{-B/2}{L_{\mathrm{h}}-1}}\right)\sum_{m=1}^{L_{\mathrm{h}}}\sigma_{\mathrm{h},m}^2\right) \tag{23}$$

and

$$\underset{L_{\mathrm{v}}}{\text{maximize}} \left(\sigma_{\mathrm{v},1}^2, \left(1-2^{\frac{-B/2}{L_{\mathrm{v}}-1}}\right)\sum_{k=1}^{L_{\mathrm{v}}}\sigma_{\mathrm{v},k}^2\right). \tag{24}$$

In (23) and (24), $1-2^{\frac{-B/2}{L_{\mathrm{h}}-1}}$ and $1-2^{\frac{-B/2}{L_{\mathrm{v}}-1}}$ are valid only when $L_{\mathrm{h}} > 1$ and $L_{\mathrm{v}} > 1$, thereby $\sigma_{\mathrm{h},1}^2$ and $\sigma_{\mathrm{v},1}^2$ are used for $L_{\mathrm{h}} = 1$ and $L_{\mathrm{v}} = 1$, respectively. As in [32], we use the exhaustive search method to find the solutions of (23) and (24) which are denoted as $\hat{L}_{\mathrm{h}}$ and $\hat{L}_{\mathrm{v}}$, respectively.

Based on $\hat{L}_{\mathrm{h}}$ and $\hat{L}_{\mathrm{v}}$, we find the numbers of feedback bits for the horizontal and vertical-domain codewords $\mathbf{f}_{L_{\mathrm{h}}}$ and $\mathbf{f}_{L_{\mathrm{v}}}$. We define the solutions for the feedback bit allocation as $\hat{B}_{\mathrm{h}}$ and $\hat{B}_{\mathrm{v}}$ which are the numbers of feedback bits for $\mathbf{f}_{L_{\mathrm{h}}}$ and $\mathbf{f}_{L_{\mathrm{v}}}$, respectively. If both $\hat{L}_{\mathrm{h}}$ and $\hat{L}_{\mathrm{v}}$ are 1, precoding at the BS is not required. Therefore, both $\mathbf{f}_{L_{\mathrm{h}}}$ and $\mathbf{f}_{L_{\mathrm{v}}}$ are not needed to be fed back, which results $\hat{B}_{\mathrm{h}} = \hat{B}_{\mathrm{v}} = 0$. Also, if $\hat{L}_{\mathrm{h}} = 1$ and $\hat{L}_{\mathrm{v}} > 1$, $\hat{B}_{\mathrm{h}} = 0$ and $\hat{B}_{\mathrm{v}} = B$, which means all feedback bits can be allocated to feeding back $\mathbf{f}_{L_{\mathrm{v}}}$. Likewise, if $\hat{L}_{\mathrm{v}} = 1$ and $\hat{L}_{\mathrm{h}} > 1$, $\hat{B}_{\mathrm{v}} = 0$ and $\hat{B}_{\mathrm{h}} = B$. Otherwise, if both $\hat{L}_{\mathrm{h}} > 1$ and $\hat{L}_{\mathrm{v}} > 1$, we can formulate an optimization problem to find B_{h} and B_{v} where

$$\underset{B_{\mathrm{h}},B_{\mathrm{v}}\in[1,\mathbb{R}^+\}}{\text{maximize}} \left(1-2^{\frac{-B_{\mathrm{h}}}{\hat{L}_{\mathrm{h}}-1}}\right)\left(1-2^{\frac{-B_{\mathrm{v}}}{\hat{L}_{\mathrm{v}}-1}}\right)\sum_{m=1}^{\hat{L}_{\mathrm{h}}}\sigma_{\mathrm{h},m}^2\sum_{k=1}^{\hat{L}_{\mathrm{v}}}\sigma_{\mathrm{v},k}^2 \tag{25a}$$

$$\text{subject to } B_{\mathrm{h}} + B_{\mathrm{v}} = B. \tag{25b}$$

In (25a), to obtain the closed-form solutions, the integer constraint on B_{h} and B_{v} is relaxed to the real number more than 1. Also, in (25a), the terms $\sum_{m=1}^{\hat{L}_{\mathrm{h}}}\sigma_{\mathrm{h},m}^2$ and $\sum_{k=1}^{\hat{L}_{\mathrm{v}}}\sigma_{\mathrm{v},k}^2$ have constant values. Therefore, the optimization problem in (25a) can be rewritten as

$$\underset{B_{\mathrm{h}},B_{\mathrm{v}}\in[1,\mathbb{R}^+\}}{\text{maximize}} \left(1-2^{\frac{-B_{\mathrm{h}}}{\hat{L}_{\mathrm{h}}-1}}\right)\left(1-2^{\frac{-B_{\mathrm{v}}}{\hat{L}_{\mathrm{v}}-1}}\right) \tag{26a}$$

$$\text{subject to } B_{\mathrm{h}} + B_{\mathrm{v}} = B. \tag{26b}$$

To obtain closed-form solutions, we reformulate the optimization problem in (26a) based on the following lemma:

Lemma 2: The optimal solution to maximize $(1-a-b+ab)$ can be found by solving

$$\text{minimize} \left(\frac{1}{a}+\frac{1}{b}\right).$$

Proof: See Appendix B. ■

Based on Lemma 2, we can reformulate the optimization problem in (26a) as

$$\underset{B_{\mathrm{h}},B_{\mathrm{v}}\in[1,\mathbb{R}^+\}}{\text{minimize}} \; 2^{\frac{B_{\mathrm{h}}}{\hat{L}_{\mathrm{h}}-1}} + 2^{\frac{B_{\mathrm{v}}}{\hat{L}_{\mathrm{v}}-1}} \tag{27a}$$

$$\text{subject to } B_{\mathrm{h}} + B_{\mathrm{v}} = B. \tag{27b}$$

The optimization problem in (27a) is convex with respect to B_{h} and B_{v} [35]. To solve the optimization problem in (27a), the Lagrangian function can be constructed as

$$\mathcal{L}(B_{\mathrm{h}}, B_{\mathrm{v}}, \lambda) = 2^{\frac{B_{\mathrm{h}}}{\hat{L}_{\mathrm{h}}-1}} + 2^{\frac{B_{\mathrm{v}}}{\hat{L}_{\mathrm{v}}-1}} + \lambda(B - B_{\mathrm{h}} - B_{\mathrm{v}}), \tag{28}$$

where λ is the Lagrange multiplier. Using (28), the Karush-Kuhn-Tucker conditions for the optimization problem in (27a) are obtained as

$$\frac{\partial\mathcal{L}(B_{\mathrm{h}}, B_{\mathrm{v}}, \lambda)}{\partial B_{\mathrm{h}}} = \frac{\ln 2}{\hat{L}_{\mathrm{h}}-1}2^{\frac{B_{\mathrm{h}}}{\hat{L}_{\mathrm{h}}-1}} + \lambda = 0, \tag{29a}$$

$$\frac{\partial\mathcal{L}(B_{\mathrm{h}}, B_{\mathrm{v}}, \lambda)}{\partial B_{\mathrm{v}}} = \frac{\ln 2}{\hat{L}_{\mathrm{v}}-1}2^{\frac{B_{\mathrm{v}}}{\hat{L}_{\mathrm{v}}-1}} + \lambda = 0, \tag{29b}$$

$$\frac{\partial\mathcal{L}(B_{\mathrm{h}}, B_{\mathrm{v}}, \lambda)}{\partial \lambda} = B - B_{\mathrm{h}} - B_{\mathrm{v}} = 0. \tag{29c}$$

By solving (29a), (29b), and (29c), the solutions are obtained as

$$\hat{B}_{\mathrm{h}} = \frac{\hat{L}_{\mathrm{h}}-1}{\hat{L}_{\mathrm{h}}+\hat{L}_{\mathrm{v}}-2}B + \frac{(\hat{L}_{\mathrm{h}}-1)(\hat{L}_{\mathrm{v}}-1)}{\hat{L}_{\mathrm{h}}+\hat{L}_{\mathrm{v}}-2}\log_2\frac{\hat{L}_{\mathrm{h}}-1}{\hat{L}_{\mathrm{v}}-1} \tag{30}$$

and

$$\hat{B}_{\mathrm{v}} = \frac{\hat{L}_{\mathrm{v}}-1}{\hat{L}_{\mathrm{h}}+\hat{L}_{\mathrm{v}}-2}B + \frac{(\hat{L}_{\mathrm{h}}-1)(\hat{L}_{\mathrm{v}}-1)}{\hat{L}_{\mathrm{h}}+\hat{L}_{\mathrm{v}}-2}\log_2\frac{\hat{L}_{\mathrm{v}}-1}{\hat{L}_{\mathrm{h}}-1}. \tag{31}$$

Based on above optimization results, we can obtain the following remarks:

Remark 1: $\hat{L}_{\mathrm{h}}$ and $\hat{L}_{\mathrm{v}}$ are dependent of the eigenvalues of the vertical and horizontal-domain spatial correlation matrices, respectively.

Remark 2: For a given $\hat{L}_{\mathrm{h}} + \hat{L}_{\mathrm{v}}$, $\hat{B}_{\mathrm{h}}$ is larger than $\hat{B}_{\mathrm{v}}$ when $\hat{L}_{\mathrm{h}} > \hat{L}_{\mathrm{v}}$ and vice versa.

IV. PROPOSED FEEDBACK SCHEME FOR HIGHLY CORRELATED VERTICAL-DOMAIN CHANNEL

In the optimization problem (20a), the solution of L_{v} can be either $\hat{L}_{\mathrm{v}} = 1$ or $\hat{L}_{\mathrm{v}} > 1$. When the vertical-domain spatial channel is highly correlated, e.g., $\sigma_{\mathrm{v},1}^2 = 1$ and $\sigma_{\mathrm{v},2}^2 = \cdots = \sigma_{\mathrm{v},L_{\mathrm{v}}}^2 = 0$, the optimal solution of L_{v} can be obtained directly as $\hat{L}_{\mathrm{v}} = 1$ [32]. This case corresponds to the channel where the vertical-domain spatial channel experiences less scattering than the horizontal-domain spatial channel [36], [37]. For example, when the height of the BS is much larger than that of the user, there are less scatterers in the vertical-domain, and then number of paths which signal passes through can be negligible. In this case, the rank of the vertical-domain spatial channel is close to 1, which implies that the vertical-domain channel is highly correlated. Such a

highly correlated vertical-domain channel environment motivates to develop more efficient feedback scheme for the KP codebook with reduced feedback and pilot overhead.

It is assumed that the rank of the vertical-domain spatial correlation matrix is 1, that is, $\mathbf{R}_{\mathrm{v}}$ is the rank-1 matrix ($r_{\mathrm{v}} = 1$), as in [29]. Accordingly, (3) can be expressed as

$$\mathbf{h} = \mathbf{h}_{\mathrm{h}} \otimes \tilde{\sigma}_{\mathrm{v},1}\mathbf{u}_{\mathrm{v},1}, \tag{32}$$

where $\mathbf{h}_{\mathrm{h}} = \mathbf{U}_{\mathrm{h}}\mathbf{\Lambda}_{\mathrm{h}}^{1/2}\mathbf{G}^{T}$, and $\mathbf{G}$ is defined in Appendix A. Substituting (32) into $\left|\mathbf{h}^{H}\left(\mathbf{f}_{\mathrm{h}} \otimes \mathbf{f}_{\mathrm{v}}\right)\right|^2$, $\left|\mathbf{h}^{H}\left(\mathbf{f}_{\mathrm{h}} \otimes \mathbf{f}_{\mathrm{v}}\right)\right|^2$ can be written as follows:

$$\begin{aligned}\left|\mathbf{h}^{H}\left(\mathbf{f}_{\mathrm{h}} \otimes \mathbf{f}_{\mathrm{v}}\right)\right|^2 &= \left|\left(\mathbf{h}_{\mathrm{h}}^{H}\mathbf{f}_{\mathrm{h}}\right)\tilde{\sigma}_{\mathrm{v},1}\left(\mathbf{u}_{\mathrm{v},1}^{H}\mathbf{f}_{\mathrm{v}}\right)\right|^2 \\ &= \left|\mathbf{h}_{\mathrm{h}}^{H}\mathbf{f}_{\mathrm{h}}\right|^2\left|\tilde{\sigma}_{\mathrm{v},1}\mathbf{u}_{\mathrm{v},1}^{H}\mathbf{f}_{\mathrm{v}}\right|^2.\end{aligned} \tag{33}$$

Substituting (33) into (6), (6) can be decomposed into

$$\mathbf{f}_{\mathrm{h}} = \underset{\tilde{\mathbf{f}}_{\mathrm{h}} \in \mathcal{C}_{\mathrm{h}}}{\arg\max}\left|\mathbf{h}_{\mathrm{h}}^{H}\tilde{\mathbf{f}}_{\mathrm{h}}\right|^2 \tag{34}$$

and

$$\mathbf{f}_{\mathrm{v}} = \underset{\tilde{\mathbf{f}}_{\mathrm{v}} \in \mathcal{C}_{\mathrm{v}}}{\arg\max}\left|\mathbf{u}_{\mathrm{v},1}^{H}\tilde{\mathbf{f}}_{\mathrm{v}}\right|^2. \tag{35}$$

The equations (34) and (35) indicate that the horizontal-domain codeword is selected based on $\mathbf{h}_{\mathrm{h}}$ which includes $\mathbf{R}_{\mathrm{h}}$ and $\mathbf{g}$, whereas the vertical-domain codeword is selected based only on $\mathbf{R}_{\mathrm{v}}$. Compared with $\mathbf{h}_{\mathrm{h}}$, $\mathbf{R}_{\mathrm{v}}$ varies at a much slower rate [28]. Therefore, the feedback periodicity of the vertical-domain codeword can become longer when $r_{\mathrm{v}} = 1$ compared with when $r_{\mathrm{v}} > 1$. Then, the feedback overhead can be reduced by longer feedback periodicity.

With the proposed feedback scheme based on (34) and (35), the pilot overhead for downlink channel estimation at the user can also be reduced. For the user to estimate the channel $\mathbf{h}$ with a dimension of N, the BS must transmit N orthogonal pilots using N symbols [38]. However, using the proposed feedback scheme based on (34) and (35), the user only estimates the channel $\mathbf{h}_{\mathrm{h}}$ which has a dimension of N_{h} smaller than N. Then, the BS transmits N_{h} orthogonal pilots, therefore, the required number of pilot symbols is reduced to N_{h}.

Next, we prove that N-dimensional channel can be obtained by transmitting only N_{h} orthogonal pilots. To reduce the dimension of the pilots from N to N_{h}, a precoded pilot is transmitted to the user. The vertical-domain precoder obtained from (35) is expressed as follows:

$$\begin{aligned}\mathbf{f}_{\mathrm{v}} &= \left[\,\hat{u}_{\mathrm{v},1}\ \hat{u}_{\mathrm{v},2}\ \cdots\ \hat{u}_{\mathrm{v},N_{\mathrm{v}}}\,\right]^{T} \\ &= a\mathbf{u}_{\mathrm{v}} + b\mathbf{u}_{\mathrm{v}}^{\perp},\end{aligned} \tag{36}$$

where $a = e^{j\varphi}\cos\varphi$, $b = 1 - \cos\varphi$, φ is the angle between $\mathbf{f}_{\mathrm{v}}$ and $\mathbf{u}_{\mathrm{v}}$ as in [39], and $\mathbf{u}_{\mathrm{v}}^{\perp}$ is a vector orthogonal to $\mathbf{u}_{\mathrm{v}}$. The precoder for the pilot is then generated using (36), which is expressed as

$$\mathbf{W}_{\mathrm{p}} = \mathbf{I}_{N_{\mathrm{h}}} \otimes \mathbf{f}_{\mathrm{v}}. \tag{37}$$

Subsequently, the pilot is precoded using $\mathbf{W}_{\mathrm{p}}$. The received pilot signal for the user can be expressed as

$$\mathbf{y} = p_{\mathrm{p}}\mathbf{h}^{H}\mathbf{W}_{\mathrm{p}}\Psi + \mathbf{n}, \tag{38}$$

where p_{p} is the pilot transmission power, Ψ is $N_{\mathrm{h}} \times N_{\mathrm{h}}$ pilot symbol matrix that satisfies $\Psi\Psi^{H} = \mathbf{I}_{N_{\mathrm{h}}}$, and $\mathbf{n}$ is an additive white Gaussian noise vector with zero mean and variance N_0.

By substituting (32) and (37) into $\mathbf{h}^{H}\mathbf{W}_{\mathrm{p}}$ in (38), $\mathbf{h}^{H}\mathbf{W}_{\mathrm{p}}$ can be written as

$$\begin{aligned}\mathbf{h}^{H}\mathbf{W}_{\mathrm{p}} &= \left(\mathbf{h}_{\mathrm{h}}^{H} \otimes \tilde{\sigma}_{\mathrm{v},1}\mathbf{u}_{\mathrm{v},1}^{H}\right)\left(\mathbf{I}_{N_{\mathrm{h}}} \otimes \mathbf{w}_{\mathrm{v}}\right) \\ &\overset{(b)}{=} \left(\mathbf{h}_{\mathrm{h}}^{H}\mathbf{I}_{N_{\mathrm{h}}}\right) \otimes \left(\tilde{\sigma}_{\mathrm{v},1}\mathbf{u}_{\mathrm{v},1}^{H}\mathbf{w}_{\mathrm{v}}\right),\end{aligned} \tag{39}$$

where (b) results from $(\mathbf{A} \otimes \mathbf{B})(\mathbf{C} \otimes \mathbf{D}) = \mathbf{AC} \otimes \mathbf{BD}$ as in [33]. By substituting (36) into (39), (39) can be expressed as follows:

$$\mathbf{h}^{H}\mathbf{W}_{\mathrm{p}} = e^{j\varphi}\cos\varphi\tilde{\sigma}_{\mathrm{v},1}\mathbf{h}_{\mathrm{h}}^{H}.$$

Furthermore, assuming perfect channel estimation at the user, $\mathbf{h}_{\mathrm{h}}$ can be estimated as follows:

$$\overline{\mathbf{h}}_{\mathrm{h}} = e^{j\varphi}\cos\varphi\tilde{\sigma}_{\mathrm{v},1}\mathbf{h}_{\mathrm{h}}. \tag{40}$$

Then, the user can select the horizontal-domain codeword as

$$\begin{aligned}\mathbf{f}_{\mathrm{h}} &= \underset{\tilde{\mathbf{f}}_{\mathrm{h}} \in \mathcal{C}_{\mathrm{h}}}{\arg\max}\left|\overline{\mathbf{h}}_{\mathrm{h}}^{H}\tilde{\mathbf{f}}_{\mathrm{h}}\right|^2 \\ &= \underset{\tilde{\mathbf{f}}_{\mathrm{h}} \in \mathcal{C}_{\mathrm{h}}}{\arg\max}\left((e^{-j\varphi}\cos\varphi)^2\tilde{\sigma}_{\mathrm{v},1}^2\left|\mathbf{h}_{\mathrm{h}}^{H}\tilde{\mathbf{f}}_{\mathrm{h}}\right|^2\right) \\ &= \underset{\tilde{\mathbf{f}}_{\mathrm{h}} \in \mathcal{C}_{\mathrm{h}}}{\arg\max}\left|\mathbf{h}_{\mathrm{h}}^{H}\tilde{\mathbf{f}}_{\mathrm{h}}\right|^2.\end{aligned} \tag{41}$$

The equation (41) is equivalent to (34). Because the selected horizontal-domain codeword can be fed back by estimating $\mathbf{h}_{\mathrm{h}}$ using the precoded pilot $\mathbf{W}_{\mathrm{p}}\Psi$, the pilot overhead can be reduced.

V. SIMULATION RESULTS

In this section, we provide the simulation results to verify the proposed schemes. First, we compare the performance of the proposed feedback bit allocation scheme with that of the fixed feedback bit allocation scheme. Next, we investigate the performance of the proposed feedback scheme for a highly correlated vertical-domain channel and compare it with the conventional feedback schemes.

To evaluate the feedback schemes with various correlation values, we consider the spatial correlation matrix represented by the exponential model, as in [40] and [41]. According to [40] and [41], the entries of the horizontal-domain spatial correlation matrix are expressed as

$$\mathbf{R}_{\mathrm{h}}(i,j) = \rho_{\mathrm{h}}^{|i-j|},$$

where $\mathbf{R}_{\mathrm{h}}(i,j)$ is the entry in the ith row and jth column of the horizontal-domain spatial correlation matrix $\mathbf{R}_{\mathrm{h}}$ and ρ_{h} is the correlation coefficient of $\mathbf{R}_{\mathrm{h}}$ with $0 \le \rho_{\mathrm{h}} \le 1$. Similarly, the

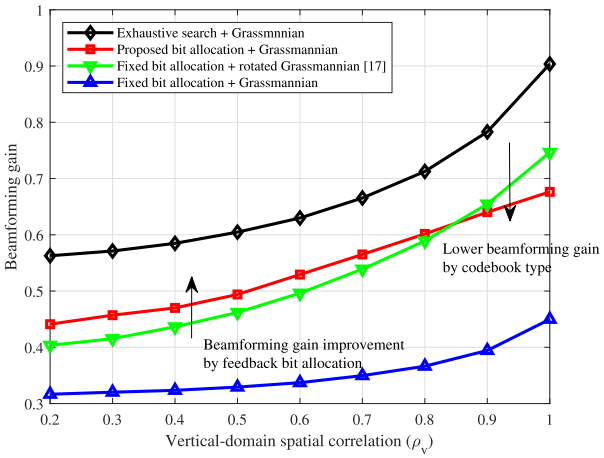

FIGURE 1. Average beamforming gain as a function of the vertical-domain spatial correlation coefficient with $N_h = N_v = 4$, $\rho_h = 0.57$, and $B = 8$.

entries of the vertical-domain spatial correlation matrix are expressed as

$$\mathbf{R}_v(i,j) = \rho_v^{|i-j|},$$

where $\mathbf{R}_v(i,j)$ is the entry in the ith row and jth column of the vertical-domain spatial correlation matrix $\mathbf{R}_v$ and ρ_v is the correlation coefficient of $\mathbf{R}_v$ with $0 \leq \rho_v \leq 1$.

A. EVALUATION OF THE PROPOSED FEEDBACK BIT ALLOCATION

In this subsection, we evaluate the proposed feedback bit allocation scheme in (30) and (31) and compare it with the fixed feedback bit allocation. The fixed feedback bit allocation always uses $B_h = B_v = B/2$, whereas the proposed scheme uses B_h and B_v which are described in Section III-B. In the simulation, we apply the Grassmannian codebook which is widely known as an effective quantization method for correlated channels [10]. We also consider the KP codebook based on the rotated Grassmannian codebook where the entries of the codebook are transformed by the square root of the horizontal and vertical-domain channel correlation matrices [17].

The average normalized beamforming gain is considered as a performance metric, which is defined as [27]

$$\mathbb{E}\left[\frac{\left|\mathbf{h}^H(\mathbf{f}_h \otimes \mathbf{f}_v)\right|^2}{\|\mathbf{h}\|^2}\right].$$

Fig. 1 shows the average normalized beamforming gains as a function of the vertical-domain spatial correlation coefficient ρ_v with $N_h = N_v = 4$ and $B = 8$. The horizontal-domain spatial correlation coefficient ρ_h is fixed to 0.57 assuming that the transmission antennas in the horizontal domain are equally separated by the distance of the two wavelengths [32]. As a benchmark, we consider the exhaustive search method that can provide the optimal solution to (20a). As shown in Fig. 1, the proposed feedback bit allocation scheme achieves about 38% $\sim$ 49% gain compared with the fixed bit allocation with the Grassmannian codebook. It is also observed that the proposed feedback bit allocation scheme outperforms the rotated Grassmannian codebook method when $\rho_v \leq 0.85$. However, the rotated Grassmannian codebook is better than the proposed feedback bit allocation when $\rho_v > 0.85$, because the beamforming gain of the rotated Grassmannian codebook increases for higher spatial correlation.

Fig. 2 shows the average normalized beamforming gains as a function of the vertical-domain spatial correlation coefficient ρ_v with $N_h = N_v = 8$ and $B = 18$. As another benchmark representing the advanced KP codebook, we consider the LC-based KP codebook (LC codebook) proposed in [23]. Instead, we omit the exhaustive search method considering the infeasible codeword search complexity when $B = 18$. Similar to Fig. 1, the proposed feedback bit allocation scheme is better than the fixed bit allocation with the Grassmannian codebook. Also, it is observed that the proposed feedback bit allocation scheme outperforms the rotated Grassmannian codebook method when $\rho_v \leq 0.85$. The LC codebook is inferior to both the proposed feedback bit allocation scheme and fixed bit allocation with the rotated Grassmannian codebook, because 18-bit LC codebook is less accurate to represent the channel than the proposed feedback bit allocation and rotated Grassmannian codebook.

Fig. 3 shows the average normalized beamforming gains as a function of the number of antennas in the vertical-domain with $N_h = 8$ and $B = 8$. ρ_v and ρ_h are fixed to 0.57 assuming that the transmission antennas in the horizontal and vertical-domains are equally separated by the distance between the two wavelengths [32]. The proposed feedback scheme shows approximately 23% $\sim$ 65% performance gain compared with the fixed bit allocation with the rotated Grassmannian codebook. This result implies that the proposed feedback bit allocation scheme with the KP codebook can improve the normalized beamforming gain by jointly optimizing the channel dimension and number of feedback bits based on the horizontal and vertical-domain spatial correlation matrices.

Fig. 4 shows the average normalized beamforming gains as a function of the number of antennas in the vertical-domain with $N_h = 8$ and $B = 18$. Similar to Fig. 3, the proposed feedback bit allocation scheme outperforms the fixed feedback bit allocation for all N_v. Further, the proposed feedback bit allocation shows better beamforming gain than the LC codebook for all N_v. This is because the channel quantization accuracy of the 18-bit LC codebook is lower than that of the Grassmannian codebook. Moreover, the LC codebook does not utilize the gain from the adaptive feedback bit allocation. Therefore, it can be inferred that the LC codebook cannot outperform the proposed feedback bit allocation scheme and Grassmannian codebook under 18-bit feedback.

From Figs. 1–4, we can conclude that the beamforing gain of the proposed feedback bit allocation scheme depends on the vertical-domain spatial correlation. In specific, we can observe from Fig. 1 that when the vertical-domain spatial

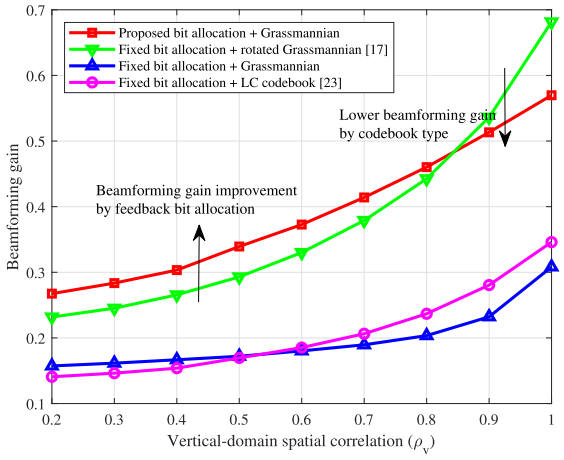

FIGURE 2. Average beamforming gain as a function of the vertical-domain spatial correlation coefficient with $N_h = N_v = 8$, $\rho_h = 0.57$, and $B = 18$.

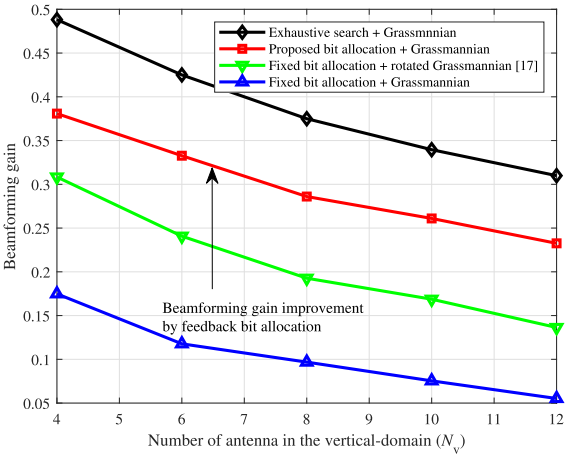

FIGURE 3. Average beamforming gain as a function of the number of antennas in the vertical-domain with $N_h = 8$ and $B = 8$.

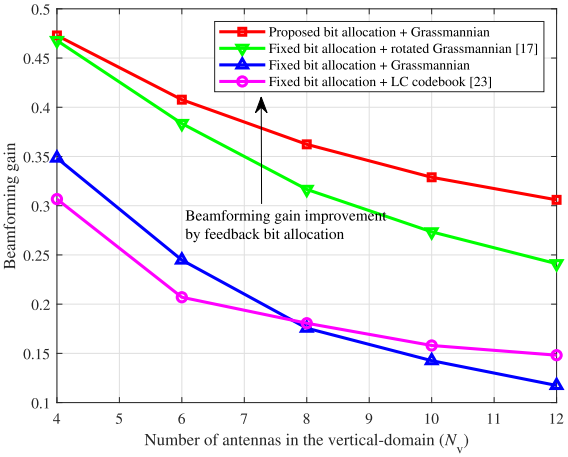

FIGURE 4. Average beamforming gain as a function of the number of antennas in the vertical-domain with $N_h = 8$ and $B = 18$.

correlation coefficient is larger than 0.85, the proposed feedback bit allocation scheme has lower beamforming gain than the rotated Grassmannian codebook with the fixed bit allocation. This is because the rotated Grassmannian codebook makes the codebook more aligned to the channel as spatial correlation coefficient becomes larger, whereas the proposed feedback bit allocation scheme does not improve the beamforming gain by modifying the codebook. Nevertheless, when the vertical-domain spatial correlation coefficient is low, the proposed feedback bit allocation scheme can bring performance gain by effectively allocating the feedback bits to the horizontal and vertical-domain codebooks. Moreover, because the horizontal and vertical-domain spatial correlation matrices are symmetrical, we can easily infer that the beamforming gain of the proposed bit allocation scheme also depends on the horizontal-domain spatial correlation coefficient.

B. EVALUATION OF THE PROPOSED FEEDBACK SCHEME

In this subsection, we compare the proposed feedback scheme with the conventional feedback schemes proposed in [27] and [30] in which both the horizontal and vertical-domain codewords are fed back. As in Section V-A, the LC codebook in [23] are also compared when $B = 18$. Also, as a baseline, we plot the ergodic rate of the perfect CSI at the transmitter (CSIT) which has no channel quantization error and pilot overhead.

Here, the ergodic rate is considered as a performance metric, which is defined as

$$R = \mathbb{E}\left[\left(1 - \frac{\tau}{T}\right)\log_2\left(1 + \frac{p}{N_0}\left|\mathbf{h}^H\left(\mathbf{f}_v \otimes \mathbf{f}_h\right)\right|^2\right)\right],$$

where $T = B_c T_c$ is the length of the coherence block with B_c coherence bandwidth and T_c coherence time, and τ is the length of the pilot for the downlink channel estimation. In the simulation, we consider $\frac{p}{N_0} = 0$ dB and $T = 180$ where the coherence bandwidth is 180kHz and the coherence time is 1ms. Furthermore, $\tau = N$ for the conventional schemes and $\tau = N_h$ for the proposed scheme.

Fig. 5 demonstrates the ergodic rates as a function of ρ_v when $N_h = N_v = 4$ and $B = 8$. The ergodic rates based on the CSI feedback are always lower than the perfect CSIT due to the quantized CSI and pilot overhead. In addition, the ergodic rates of all feedback schemes increase as ρ_v increases, because the diversity gain increases as ρ_v increases. In Fig. 5a, when $\rho_v < 0.35$ with $\rho_h = 0.1$, the conventional feedback schemes outperform the proposed feedback scheme because the small-scale fading channel is not accurately compressed to $\mathbf{f}_h$. However, when $\rho_v \geq 0.35$, the proposed feedback scheme outperforms the conventional feedback schemes. As ρ_v increases, the vertical-domain spatial correlation matrix can be more separated from the horizontal-domain spatial correlation matrix and small-scale fading channel, as analyzed in Section IV. The proposed scheme compresses the vertical-domain spatial correlation matrix into the vertical-domain codeword only, and the horizontal-domain codeword does not include the vertical-domain spatial correlation matrix. In contrast,

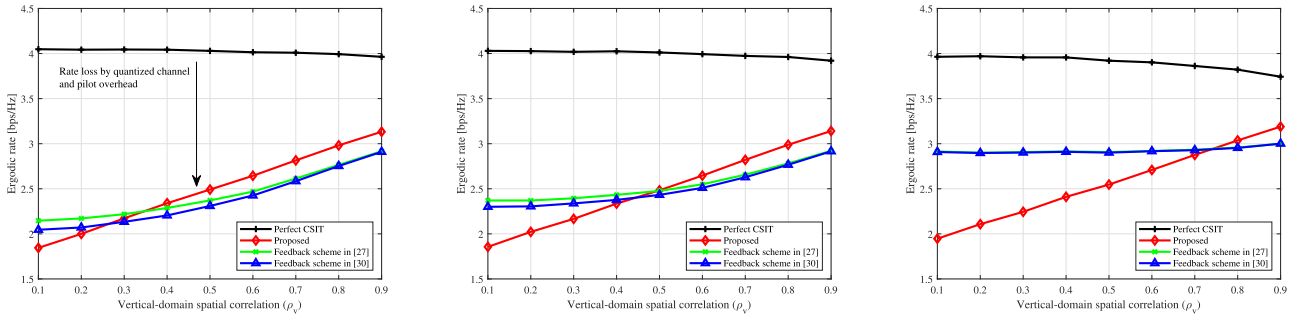

(a) $\rho_h = 0.1$ (b) $\rho_h = 0.5$ (c) $\rho_h = 0.9$

FIGURE 5. Ergodic rate as a function of ρ_v for $N_h = N_v = 4$ and $B = 8$.

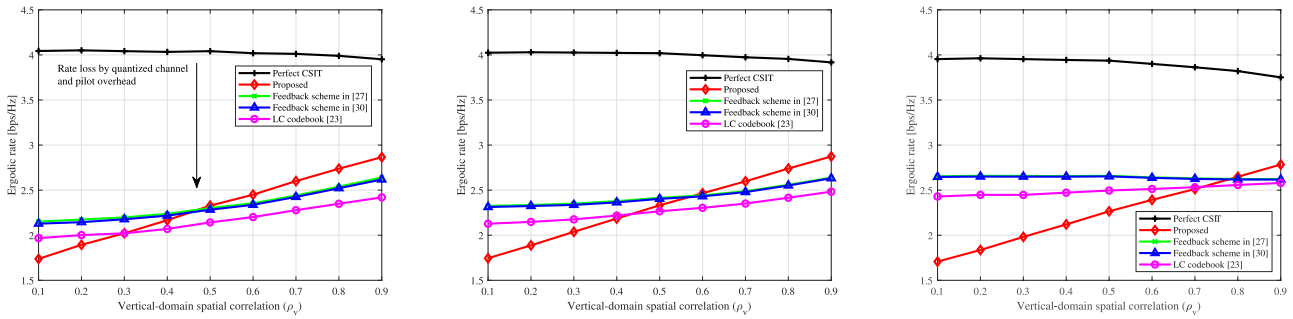

(a) $\rho_h = 0.1$ (b) $\rho_h = 0.5$ (c) $\rho_h = 0.9$

FIGURE 6. Ergodic rate as a function of ρ_v for $N_h = N_v = 4$ and $B = 18$.

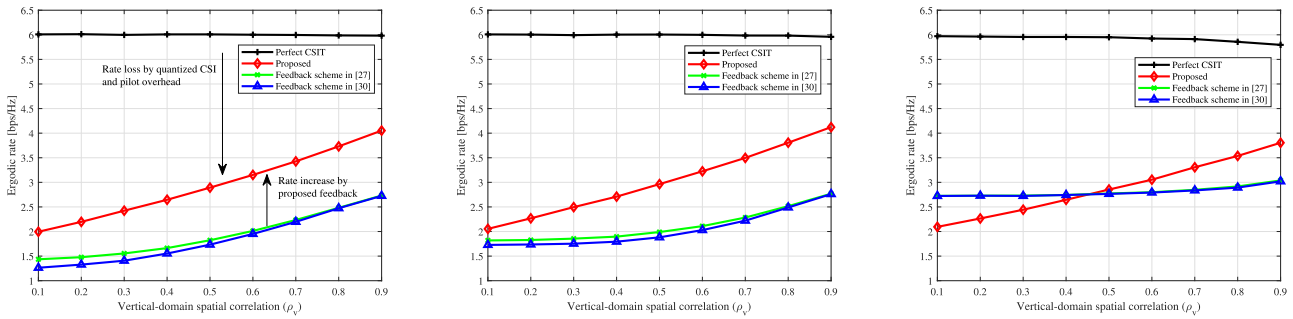

(a) $\rho_h = 0.1$ (b) $\rho_h = 0.5$ (c) $\rho_h = 0.9$

FIGURE 7. Ergodic rate as a function of ρ_v for $N_h = N_v = 8$ and $B = 8$.

the conventional schemes compress the vertical-domain spatial correlation matrix to both the horizontal and vertical-domain codewords, which leads to inaccurate feedback for the vertical-domain spatial correlation matrix. Therefore, the proposed scheme is better than the conventional schemes with larger ρ_v because of more accurate compression of the vertical-domain spatial correlation matrix. We also compare the results when $\rho_h = 0.1, 0, 5$, and 0.9. As ρ_h increases, the conventional feedback schemes achieve a larger gain of the ergodic rate than the proposed scheme, because the accuracy of compressing horizontal-domain spatial correlation matrix is not guaranteed in the proposed scheme.

Fig. 6 illustrates the ergodic rates as a function of ρ_v when $N_h = N_v = 4$ and $B = 18$. Similar to Fig. 5, when $B = 18$, the proposed feedback scheme also outperforms the conventional schemes for the large ρ_v regime. However, the LC codebook is inferior to the conventional feedback schemes for all ρ_h and ρ_v. Further, because the LC codebook requires transmitting pilot for all antennas, the gain from the reduced pilot overhead cannot be obtained. Therefore, it can be inferred from Fig. 6 that the proposed scheme can obtain the performance gain compared with the LC codebook in terms of the ergodic rate.

Fig. 7 shows the ergodic rates as a function of ρ_v when $N_h = N_v = 8$ and $B = 8$. As shown in Fig. 7, the ergodic

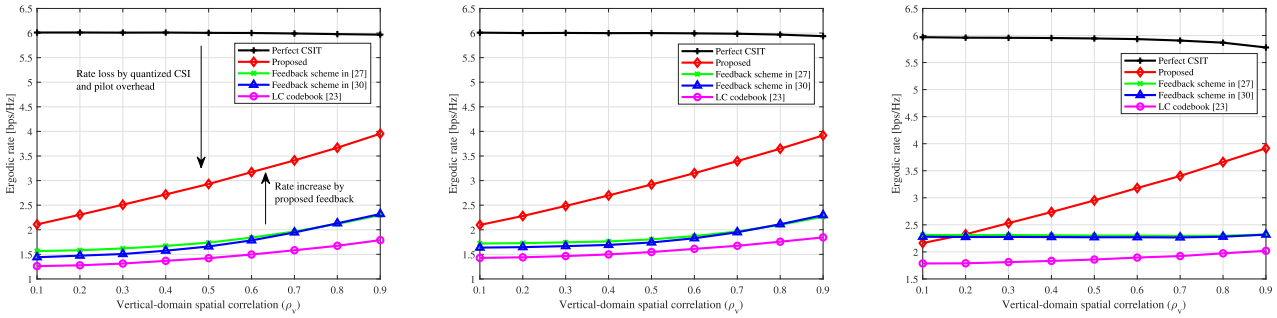

(a) $\rho_h = 0.1$ (b) $\rho_h = 0.5$ (c) $\rho_h = 0.9$

FIGURE 8. Ergodic rate as a function of ρ_v for $N_h = N_v = 8$ and $B = 18$.

rates of all feedback schemes increase as ρ_v increases due to the increasing diversity gain for larger ρ_v. In addition, the proposed feedback scheme outperforms the conventional feedback schemes for all regions except when $\rho_v < 0.5$ with $\rho_h = 0.9$. When $\rho_v < 0.5$ with $\rho_h = 0.9$, the proposed feedback scheme is inferior to the conventional schemes due to inaccurate compression of the small-scale fading channel to $\mathbf{f}_h$. However, expect when $\rho_v < 0.5$ with $\rho_h = 0.9$, the reduced pilot overhead can provide the rate gain to the proposed feedback scheme. While conventional feedback schemes require $\tau = N = 64$ pilots to estimate the downlink channel at the user, the proposed scheme transmits only $\tau = N_h = 8$ pilots to estimate the downlink channel.[1] As a result, the proposed feedback scheme can achieve a 48% rate gain by the reduced pilot overhead.

Fig. 8 describes the ergodic rates as a function of ρ_v when $N_h = N_v = 8$ and $B = 18$. The proposed feedback scheme outperforms the conventional feedback schemes except when $\rho_v < 0.2$ with $\rho_h = 0.9$. Compared with Fig. 7, the region where the proposed feedback scheme is inferior to the conventional feedback schemes is reduced. Since the channel quantization loss becomes larger with increased N_h and N_v, the gain from the reduced pilot overhead becomes more dominant in $N_h = N_v = 8$ than $N_h = N_v = 4$. Further, contrary to Fig. 6, the LC codebook shows lower ergodic rate than the proposed and conventional feedback schemes for all ρ_h and ρ_v. This is because the channel quantization error of the LC codebook is much severe for larger N_h and N_v than the other feedback schemes, thereby becoming the impact of the large pilot overhead more dominant. Therefore, the proposed feedback scheme can obtain more rate gain for larger N_h and N_v compared with the LC codebook, which cannot utilize its advanced channel quantization structure.

From Figs. 5–8, we can conclude that the performance of the proposed feedback scheme depends on the vertical-domain spatial correlation coefficient. As the vertical-domain spatial correlation coefficient becomes larger, the proposed feedback scheme finds the vertical-domain precoder more aligned to the first eigenvector of the vertical-domain spatial correlation matrix. In addition, the selected horizontal-domain precoder can compress small-scale fading channel more accurately, as the vertical-domain spatial correlation coefficient becomes larger. However, as the vertical-domain spatial correlation coefficient becomes smaller, the selected horizontal and vertical-domain precoders become less close the channel $\mathbf{h}$. The vertical-domain precoder can only represent the first eigenvector of the vertical-domain spatial correlation matrix. Then, remaining channel component except $\mathbf{h}_h \otimes \sigma_{v,1}\mathbf{u}_{v,1}$, $\sum_{k=2}^{r_v} \left(\mathbf{h}_h \otimes \sigma_{v,k}\mathbf{u}_{v,k}\right)$, is not included to both horizontal and vertical-domain precoders, which means that the remaining channel component becomes larger as the vertical-domain spatial correlation coefficient becomes smaller. Therefore, the selected horizontal and vertical-domain precoders become inaccurate.

[1] In the simulation, we omit the pilot overhead for $\mathbf{f}_v$ because the overhead for $\mathbf{f}_v$ can be ignored considering that $\mathbf{R}_v$ changes much slower than $\mathbf{h}_h$.

VI. CONCLUSION

In this study, we have proposed limited feedback designs for the KP codebook in massive MIMO systems using UPA structure. First, we have proposed a feedback bit allocation scheme that considers the horizontal and vertical-domain spatial correlation matrices. We have formulated and solved an optimization problem to maximize the average beamforming gain in terms of the number of feedback bits. Second, we have proposed a feedback scheme for highly correlated vertical-domain channel. The proposed feedback scheme reduces the feedback and pilot overhead by compressing the small-scale fading channel into a horizontal-domain codeword. Simulation results have shown that the proposed feedback bit allocation scheme improves the normalized beamforming gain compared with the conventional schemes with the fixed feedback bit allocation. The simulation results have also shown that the proposed feedback scheme outperforms the conventional feedback schemes in terms of the ergodic rate.

APPENDIX A
PROOF OF LEMMA 1

Let $\mathbf{A} = [\mathbf{a}_1, \mathbf{a}_2, \cdots \mathbf{a}_n]$ be an $m \times n$ matrix where $\mathbf{a}_j$ is the jth column vector for $j = 1, \cdots, n$. Then, the $mn \times 1$ column

vector col($\mathbf{A}$) is defined as

$$\text{col}(\mathbf{A}) = [\mathbf{a}_1^T, \mathbf{a}_2^T, \cdots, \mathbf{a}_n^T]^T. \tag{42}$$

Based on (42), $\mathbf{g} = \text{col}(\mathbf{G})$ where

$$\mathbf{G} = \begin{bmatrix} g_1 & g_{N_\text{v}+1} & \cdots & g_{(N_\text{h}-1)N_\text{v}+1} \\ \vdots & \vdots & \ddots & \vdots \\ g_{N_\text{v}} & g_{2N_\text{v}} & \cdots & g_{N_\text{h}N_\text{v}} \end{bmatrix}. \tag{43}$$

Then, (4) can be written as

$$\begin{aligned} \mathbf{h} &= \left[\left(\mathbf{U}_\text{h}\mathbf{\Lambda}_\text{h}^{1/2}\right) \otimes \left(\mathbf{U}_\text{v}\mathbf{\Lambda}_\text{v}^{1/2}\right)\right] \text{col}(\mathbf{G}) \\ &\overset{(c)}{=} \text{col}\left(\mathbf{U}_\text{v}\mathbf{\Lambda}_\text{v}^{1/2}\mathbf{G}\left(\mathbf{U}_\text{h}\mathbf{\Lambda}_\text{h}^{1/2}\right)^T\right) \\ &\overset{(d)}{=} \text{col}\left(\mathbf{U}_\text{v}\mathbf{\Lambda}_\text{v}^{1/2}\left(\mathbf{U}_\text{h}\mathbf{\Lambda}_\text{h}^{1/2}\mathbf{G}^T\right)^T\right) \\ &= \text{col}\left(\mathbf{U}_\text{v}\mathbf{\Lambda}_\text{v}^{1/2}\begin{bmatrix} \mathbf{h}_{\text{h},1}^T \\ \vdots \\ \mathbf{h}_{\text{h},N_\text{v}}^T \end{bmatrix}\right), \end{aligned} \tag{44}$$

where $(\mathbf{C}^T \otimes \mathbf{A})\text{col}(\mathbf{B}) = \text{col}(\mathbf{ABC})$ and $(\mathbf{BA})^T = \mathbf{A}^T\mathbf{B}^T$ are applied in (c) and (d), respectively.

Let us define $h_{k,j}$ as the jth element of the vector $\mathbf{h}_{\text{h},k}$. Then, we can define $\bar{\mathbf{h}}_j = [h_{1,j}, h_{2,j}, \cdots, h_{N_\text{v},j}]^T$ for $j = 1, \cdots, N_\text{h}$, and (44) can be written as

$$\begin{aligned} \mathbf{h} &= \text{col}\left(\mathbf{U}_\text{v}\mathbf{\Lambda}_\text{v}^{1/2}\left[\,\bar{\mathbf{h}}_1 \;\cdots\; \bar{\mathbf{h}}_{N_\text{h}}\,\right]\right) \\ &= \left[\,\left(\mathbf{U}_\text{v}\mathbf{\Lambda}_\text{v}^{1/2}\bar{\mathbf{h}}_1\right)^T \;\cdots\; \left(\mathbf{U}_\text{v}\mathbf{\Lambda}_\text{v}^{1/2}\bar{\mathbf{h}}_{N_\text{h}}\right)^T\,\right]^T. \end{aligned} \tag{45}$$

In (45), $\mathbf{U}_\text{v}\mathbf{\Lambda}_\text{v}^{1/2}\bar{\mathbf{h}}_j$ can be written as

$$\mathbf{U}_\text{v}\mathbf{\Lambda}_\text{v}^{1/2}\bar{\mathbf{h}}_j = \sum_{k=1}^{N_\text{v}} h_{k,j}\sigma_{\text{v},k}\mathbf{u}_{\text{v},k}. \tag{46}$$

Substituting (46) into (45), (45) can be written as

$$\begin{aligned} \mathbf{h} &= \left[\left(\sum_{k=1}^{N_\text{v}} h_{k,1}\sigma_{\text{v},k}\mathbf{u}_{\text{v},k}\right)^T, \cdots, \left(\sum_{k=1}^{N_\text{v}} h_{k,N_\text{h}}\sigma_{\text{v},k}\mathbf{u}_{\text{v},k}\right)^T\right] \\ &= \sum_{k=1}^{N_\text{v}}\left[\,h_{k,1}\sigma_{\text{v},k}\mathbf{u}_{\text{v},k} \;\cdots\; h_{k,N_\text{h}}\sigma_{\text{v},k}\mathbf{u}_{\text{v},k}\,\right]^T \\ &= \sum_{k=1}^{N_\text{v}} \mathbf{h}_{\text{h},k} \otimes \sigma_{\text{v},k}\mathbf{u}_{\text{v},k}^T. \end{aligned} \tag{47}$$

(47) can be obtained from $\mathbf{h}_{\text{h},k} = [h_{k,1}, \cdots, h_{k,N_\text{h}}]$.

APPENDIX B
PROOF OF LEMMA 2

The maximum $(1-a-b+ab)$ can be achieved by minimizing a and b and maximizing ab. Then we can decompose the optimization problem to maximize $(1-a-b+ab)$ into

$$\text{minimize } (a+b) \tag{48}$$

and

$$\text{maximize } (ab). \tag{49}$$

To find a solution that satisfies (48) and (49) simultaneously, we can formulate an optimization problem given by

$$\text{minimize } \left(\frac{a+b}{ab}\right). \tag{50}$$

The objective function in (50) can be written as $(1/a + 1/b)$. This completes the proof.

REFERENCES

[1] Y. Kim, F. Sun, Y. Wang, Y. Qi, J. Lee, Y. Kim, J. Oh, H. Ji, J. Yeo, S. Choi, H. Ryu, H. Noh, and T. Kim, "New radio (NR) and its evolution toward 5G-advanced," *IEEE Wireless Commun.*, vol. 26, no. 3, pp. 2–7, Jun. 2019.

[2] E. G. Larsson, O. Edfors, F. Tufvesson, and T. L. Marzetta, "Massive MIMO for next generation wireless systems," *IEEE Commun. Mag.*, vol. 52, no. 2, pp. 186–195, Feb. 2014.

[3] F. Rusek, D. Persson, B. K. Lau, E. G. Larsson, T. L. Marzetta, O. Edfors, and F. Tufvesson, "Scaling up MIMO: Opportunities and challenges with very large antennas," *IEEE Signal Process. Mag.*, vol. 2013, no. 347, pp. 8–20, Dec. 2013.

[4] *NR; Base Station (BS) Radio Transmission and Reception (V17.6.0, Release 17)*, 3GPP, Standard TS 38.104, Jun. 2022.

[5] J. Choi, D. J. Love, and P. Bidigare, "Downlink training techniques for FDD massive MIMO systems: Open-loop and closed-loop training with memory," *IEEE J. Sel. Topics Signal Process.*, vol. 8, no. 5, pp. 802–814, Oct. 2014.

[6] A. Rajoriya, R. Budhiraja, and L. Hanzo, "Centralized and decentralized channel estimation in FDD multi-user massive MIMO systems," *IEEE Trans. Veh. Technol.*, vol. 71, no. 7, pp. 7325–7342, Jul. 2022.

[7] F. Rottenberg, T. Choi, P. Luo, C. J. Zhang, and A. F. Molisch, "Performance analysis of channel extrapolation in FDD massive MIMO systems," *IEEE Trans. Wireless Commun.*, vol. 19, no. 4, pp. 2728–2741, Jan. 2020.

[8] Z. Qin, H. Yin, Y. Cao, W. Li, and D. Gesbert, "A partial reciprocity-based channel predictrion framework for FDD massive MIMO with high mobility," *IEEE Trans. Wireless Commun.*, vol. 21, no. 11, pp. 9638–9652, Nov. 2022.

[9] D. J. Love and R. W. Heath Jr., "Limited feedback unitary precoding for spatial multiplexing systems," *IEEE Trans. Inf. Theory*, vol. 51, no. 8, pp. 2967–2976, Aug. 2005.

[10] D. Love and R. W. Heath Jr., "Limited feedback diversity techniques for correlated channels," *IEEE Trans. Veh. Tech.*, vol. 55, no. 2, pp. 718–722, Mar. 2006.

[11] J. H. Lee and W. Choi, "Unified codebook design for vector channel quantization in MIMO broadcast channels," *IEEE Trans. Signal Process.*, vol. 63, no. 10, pp. 2509–2519, May 2015.

[12] Y. Zhang, M. Alrabeiah, and A. Alkhateeb, "Reinforcement learning of beam codebooks in millimeter wave and terahertz MIMO systems," *IEEE Trans. Commun.*, vol. 70, no. 2, pp. 904–919, Feb. 2022.

[13] J. Guo, C.-K. Wen, M. Chen, and S. Jin, "Environment knowledge-aided massive MIMO feedback codebook enhancement using artificial intelligence," *IEEE Trans. Commun.*, vol. 70, no. 7, pp. 4527–4542, Jul. 2022.

[14] R. C. Hansen, *Phased Array Antennas*, 2nd ed. Hoboken, NJ, USA: Wiley, 2009.

[15] G. Levin and S. Loyka, "On capacity-maximizing angular densities of multipath in MIMO channels," in *Proc. IEEE 72nd Veh. Technol. Conf. - Fall*, Ottawa, ON, Canada, Sep. 2010, pp. 1–5.

[16] J. Li, X. Su, J. Zeng, Y. Zhao, S. Yu, L. Xiao, and X. Xu, "Codebook design for uniform rectangular arrays of massive antennas," in *Proc. IEEE 77th Veh. Technol. Conf.*, Dresden, Germany, Jun. 2013, pp. 1–5.

[17] D. Ying, F. W. Vook, T. A. Thomas, D. J. Love, and A. Ghosh, "Kronecker product correlation model and limited feedback codebook design in a 3D channel model," in *Proc. IEEE Int. Conf. Commun. (ICC)*, Sydney, NSW, Australia, Jun. 2014, pp. 5865–5870.

[18] M. Mussbah, S. Pratschner, S. Schwarz, and M. Rupp, "Computationally efficient limited feedback for codebook-based FD-MIMO precoding," in *Proc. 23rd Int. ITG Workshop Smart Antennas*, Vienna, Austria, Apr. 2019, pp. 1–5.

[19] B. Özbek, C. Arslan, M. Demirtaş, H. Şahan, F. K. Kadı, and E. Elçi, "Limited feedback design for massive full dimension MIMO systems," in *Proc. Joint Eur. Conf. Netw. Commun. 6G Summit*, Grenoble, France, Jun. 2022, pp. 89–93.
[20] J. Choi, K. Lee, D. J. Love, T. Kim, and R. W. Heath Jr., "Advanced limited feedback designs for FD-MIMO using uniform planar arrays," in *Proc. IEEE Global Commun. Conf. (GLOBECOM)*, San Diego, CA, USA, Dec. 2015, pp. 1–6.
[21] J. Song, J. Choi, T. Kim, and D. J. Love, "Advanced quantizer designs for FDD-based FD-MIMO systems using uniform planar arrays," *IEEE Trans. Signal Process.*, vol. 66, no. 14, pp. 3891–3905, Jul. 2018.
[22] K. Bhogi, C. Saha, and H. S. Dhillon, "Learning on a Grassmann manifold: CSI quantization for massive MIMO systems," in *Proc. 54th Asilomar Conf. Signals, Syst., Comput.*, Pacific Grove, CA, USA, Nov. 2020, pp. 179–186.
[23] M. S. Rahman, Y.-H. Nam, J. Zhang, and J.-Y. Seol, "Linear combination codebook based CSI feedback scheme for FD-MIMO systems," in *Proc. IEEE Globecom Workshops*, San Diego, CA, USA, May 2015, pp. 1–6.
[24] B. Mondal, V. Sergeev, A. Sengupta, and A. Davydov, "5G-NR (new radio) CSI computation algorithm and performance," in *Proc. 52nd Asilomar Conf. Signals, Syst., Comput.*, Pacific Grove, CA, USA, Oct. 2018, pp. 1068–1107.
[25] C.-C. Tsai, T.-Y. Yeh, W.-H. Chou, W.-C. Pao, and J.-Y. Pan, "A low complexity PMI selection scheme for 3GPP 5G NR FDD systems," in *Proc. Asia–Pacific Signal Inf. Process. Assoc. Annu. Summit Conf.*, Tokyo, Japan, Dec. 2021, pp. 1917–1922.
[26] J. Kang, O. Simeone, J. Kang, and S. Shamai (Shitz), "Layered downlink precoding for C-RAN systems with full dimensional MIMO," *IEEE Trans. Veh. Technol.*, vol. 66, no. 3, pp. 2170–2182, Mar. 2017.
[27] J. Choi, T. Kim, D. J. Love, and J.-Y. Seol, "Exploiting the preferred domain of FDD massive MIMO systems with uniform planar arrays," in *Proc. IEEE Int. Conf. Commun. (ICC)*, London, U.K., Jun. 2015, pp. 1465–1470.
[28] A. Adhikary, J. Nam, J.-Y. Ahn, and G. Caire, "Joint spatial division and multiplexing: The large-scale array regime," *IEEE Trans. Inf. Theory*, vol. 59, no. 10, pp. 6441–6463, Oct. 2013.
[29] A. Alkhateeb, G. Leus, and R. W. Heath Jr., "Multi-layer precoding: A potential solution for full-dimensional massive MIMO systems," *IEEE Trans. Wireless Commun.*, vol. 16, no. 9, pp. 5810–5824, Sep. 2017.
[30] H. Ji, C. Shin, Y. Kim, and Y.-H. Nam, "3-dimensional channel characteristics on 2-dimensional active array antennas," in *Proc. Int. Conf. Comput., Netw. Commun. (ICNC)*, Anaheim, CA, USA, Feb. 2015, pp. 16–20.
[31] C. K. Au-Yeung and D. J. Love, "On the performance of random vector quantization limited feedback beamforming in a MISO system," *IEEE Trans. Wireless Commun.*, vol. 6, no. 2, pp. 458–462, Feb. 2007.
[32] J.-Y. Ko and Y.-H. Lee, "Adaptive beamforming with dimension reduction in spatially correlated MISO channels," *IEEE Trans. Wireless Commun.*, vol. 8, no. 10, pp. 4998–5002, Oct. 2009.
[33] M. Brookes. *The Matrix Reference Manual*. [Online]. Available: http://www.ee.imperial.ac.uk/hp/staff/dmb/matrix/intro.html
[34] S. Boyd and L. Vandenberghe, *Convex Optimization*, Cambridge, U.K.: Cambridge Univ. Press, 2004.
[35] N. Lee and W. Shin, "Adaptive feedback scheme on K-cell MISO interfering broadcast channel with limited feedback," *IEEE Trans. Wireless Commun.*, vol. 10, no. 2, pp. 401–406, Feb. 2011.
[36] N. Seifi, J. Zhang, R. W. Heath Jr., T. Svensson, and M. Coldrey, "Coordinated 3D beamforming for interference management in cellular networks," *IEEE Trans. Wireless Commun.*, vol. 13, no. 10, pp. 5396–5410, Oct. 2014.
[37] Z. Zhong, X. Yin, X. Li, and X. Li, "Extension of ITU IMT-advanced channel models for elevation domains and line-of-sight scenarios," in *Proc. IEEE 78th Veh. Technol. Conf. (VTC Fall)*, Las Vegas, NV, USA, Sep. 2013, pp. 1–5.
[38] B. Hassibi and B. M. Hochwald, "How much training is needed in multiple-antenna wireless links?" *IEEE Trans. Inf. Theory*, vol. 49, no. 4, pp. 951–963, Apr. 2003.
[39] T. Yoo, N. Jindal, and A. Goldsmith, "Multi-antenna downlink channels with limited feedback and user selection," *IEEE J. Sel. Areas Commun.*, vol. 25, no. 7, pp. 1478–1491, Sep. 2007.
[40] J. Choi and D. J. Love, "Bounds on eigenvalues of a spatial correlation matrix," *IEEE Commun. Lett.*, vol. 18, no. 8, pp. 1391–1394, Aug. 2014.
[41] H. Lim, Y. Jang, and D. Yoon, "Bounds for eigenvalues of spatial correlation matrices with the exponential model in MIMO systems," *IEEE Trans. Wireless Commun.*, vol. 16, no. 2, pp. 1196–1204, Feb. 2017.
[42] *NR; Physical Layer Procedures for Data (V17.3.0, Release 17)*, 3GPP, Standard TS 38.214, Sep. 2022.

KYUNGSIK MIN received the B.S. and Ph.D. degrees in electrical and electronic engineering from Yonsei University, Seoul, South Korea, in 2011 and 2017, respectively. From 2017 to 2023, he was a Staff Engineer with Samsung Electronics, working on the physical and MAC layer design for 5G systems. Since 2023, he has been an Assistant Professor with the Department of Information and Telecommunications Engineering, The University of Suwon, South Korea. His research interests include 5G/6G communication systems, massive MIMO systems, full-duplex radio, and mmWave communications. He was a recipient of the Global Ph.D. Fellowship from the National Research Foundation of Korea, in 2011.

TAEHYOUNG KIM (Member, IEEE) received the B.S. and Ph.D. degrees in electrical and electronic engineering from Yonsei University, Seoul, South Korea, in 2010 and 2016, respectively. From 2016 to 2021, he was a Senior Engineer with Samsung Electronics Company Ltd., where he was involved in the standardization of 5G wireless communication systems in 3GPP. From March 2021 to August 2021, he was a Senior Researcher with the Electronics and Telecommunications Research Institute (ETRI), where he was involved in the development and implementation of moving network for vehicular communication. Since September 2021, he has been an Assistant Professor with the Department of Information and Communication Engineering, Soonchunhyang University. His research interests include developing core technologies for 5G/6G communication systems, physical layer channel design, massive MIMO, and 3GPP RAN1 standardization.